ISSN 1029-9599, Physical Mesomechanics, 2021, Vol. 24, No. 6, pp. 642–652. © Pleiades Publishing, Ltd., 2021.
Russian Text © The Author(s), 2021, published in Fizicheskaya Mezomekhanika, 2021, Vol. 24, No. 4, pp. 16–27.

Design and Characterization of Al-Cr-Nb-Ti-V-Zr High-Entropy Alloys for High-Temperature Applications

N. Yu. Yurchenko[1]*, E. S. Panina[1], G. A. Salishchev[1], and N. D. Stepanov[1]

[1] *Belgorod National Research University, Belgorod, 308015 Russia*
** e-mail: yurchenko_nikita@bsu.edu.ru*

Received March 31, 2021; revised April 21, 2021; accepted April 21, 2021

Abstract—High-entropy alloys (HEAs) are a new class of metallic alloys without a principal component. These materials are attractive because of their unique structures and properties, including mechanical ones. Some of HEAs based on refractory metals are considered as advanced high-temperature materials. However, the development of new applicable compositions is complicated by poor understanding of relationships between the chemical and phase composition of HEAs and their effect on mechanical performance. Here we report the results of comprehensive studies of Al-Cr-Nb-Ti-V-Zr high-entropy alloys, particularly $AlCr_xNbTiVZr_y$ ($x = 0.00$, 0.25, 0.50, 1.00, 1.50 at $y = 0$ and $y = 0.0$, 0.25, 0.50, 1.00, 1.50 at $x = 0$). The strength and ductility of such alloys are shown to have a complex relationship with the composition and order of the parent B2 phase, and the amount and nature of secondary phases (C14 Laves phase and zirconium aluminides). Some of the investigated alloys demonstrate high specific strength at $T \leq 800$°C. $AlNbTiVZr_{0.25}$ alloy also has a stable microstructure and higher creep resistance at 600°C compared to existing creep-resistant alloys. Based on calculations of equilibrium and nonequilibrium phase diagrams by the CALPHAD method, we propose new Al-Cr-Nb-Ti-Zr alloy compositions with unique lamellar eutectic structure composed of the B2 and C14 Laves phases and with enhanced strength properties. The structure/property relationships and high-temperature deformation mechanisms of refractory HEAs with eutectic microstructure are analyzed.

Keywords: high-entropy alloys, refractory high-entropy alloys, eutectic refractory high-entropy alloys, structure, mechanical properties, creep resistance

DOI: 10.1134/S1029959921060023

1. INTRODUCTION

Metallic materials with unique properties are increasingly demanded by safety-critical industries. For example, nickel superalloys are the main structural material for the hot sections of gas turbine compressors. The maximum operating temperature of the most modern superalloys does not exceed 1200°C, and their density is more than 9 g/cm^3. A further increase in the efficiency of gas turbine engines is impossible without increasing the operating temperature and/or reducing the weight of the structure. One of the solutions to the problem is the use of new materials, e.g., the so-called high-entropy alloys or HEAs.

HEAs are multicomponent systems (of at least 4-5 elements) with nearly equiatomic concentrations of the constituent elements. Initially, HEAs as advanced high-temperature materials were based exclusively on refractory metals such as W, Mo, Ta, Nb, and V [1]. NbMoTaW and VNbMoTaW alloys had a single-phase bcc structure and exhibited high strength (>400 MPa at $T = 1600$°C), but their density was much higher (>12 g/cm^3) than that of industrial nickel superalloys [2]. In order to increase the specific strength, it was proposed to use lighter refractory elements. A Cr-Nb-Ti-V-Zr system was presented [3, 4] which gave CrNbTiVZr alloy with a density of ~6.5 g/cm^3 and a structure consisting of a bcc matrix and Laves phase particles. The alloy showed a higher specific yield strength at temperatures up to 1000°C compared to Inconel 718 and Haynes 230 superalloys. The use of light Al as an alloying element in HEAs based on refractory metals was also shown to be effective. The replacement of Cr by Al in $CrMo_{0.5}NbTa_{0.5}TiZr$ alloy led to a decrease in density from 8.2 to 7.4 g/cm^3 and an increase in specific strength at $T \leq 1000$°C [5]. The competitive mechanical properties of HEAs of the Cr-Nb-Ti-V-Zr system and the possibility of further

increasing their specific strength by introducing Al allowed the development of new compositions based on the extended Al-Cr-Nb-Ti-V-Zr system [6–11].

This paper discusses the relationship between the chemical and phase composition of HEAs of the Al-Cr-Nb-Ti-V-Zr system, and their effect on mechanical properties. It is demonstrated that the eutectic structure in alloys of this system can be correctly predicted using the CALPHAD method. The possibility of synthesizing alloys with a specific strength significantly exceeding that of industrial nickel superalloys at $T \leq 800$°C is shown.

2. MATERIALS AND METHODS

The investigation was performed on compositions $AlCr_xNbTiVZr_y$ ($x = 0.0$, 0.25, 0.5, 1.0, 1.5 at $y = 0$ and $y = 0.0$, 0.25, 0.5, 1.0, 1.5 at $x = 0$) (where x or y indicates the mole fraction of the component). Experimental studies were also conducted on compositions $Nb_{30}Ti_{40}Zr_{30}$, $Cr_{20}Nb_{30}Ti_{40}Zr_{10}$, $Al_{15}Cr_{20}Nb_{15}Ti_{40}Zr_{10}$, $Al_{23}Cr_{20}Nb_{15}Ti_{32}Zr_{10}$, $Al_{28}Cr_{20}Nb_{15}Ti_{27}Zr_{10}$, and $Al_{33}Cr_{20}Nb_{15}Ti_{22}Zr_{10}$ (the subscript indicates the content of the element in at %). The alloys were produced by vacuum arc remelting of high-purity metals (no less than 99.9 wt %) in a copper mold under argon. Ingots of $AlCr_xNbTiVZr_y$ alloy were vacuum sealed in a quartz tube (10^{-2} torr) and homogenized at $T = 1200$°C for 2 h (initial state). $Nb_{30}Ti_{40}Zr_{30}$, $Cr_{20}Nb_{30}Ti_{40}Zr_{10}$, $Al_{15}Cr_{20}Nb_{15}Ti_{40}Zr_{10}$, $Al_{23}Cr_{20}Nb_{15}Ti_{32}Zr_{10}$, $Al_{28}Cr_{20}Nb_{15}Ti_{27}Zr_{10}$, and $Al_{33}Cr_{20}Nb_{15}Ti_{22}Zr_{10}$ alloys were investigated in the as-cast state. The alloy microstructures were studied by X-ray diffraction analysis, SEM, and TEM. The degree of long-range order of the B2 phase in alloys was determined by X-ray diffraction analysis from the ratio of the intensities of superstructural and fundamental reflections, taking into account the predominant arrangement of the constituent element atoms in the sublattice sites [8]. Mechanical compression tests of alloy samples were conducted at temperatures of 22–1000°C and a strain rate of 10^{-4} s^{-1}. A more detailed description of the techniques used can be found in [6–11].

3. RESULTS AND DISCUSSION

3.1. Investigation of $AlCr_xNbTiVZr_y$ Alloys

First, we studied AlNbTiV alloy of the Al-Cr-Nb-Ti-V-Zr system. This composition was shown to have a single-phase bcc structure and a high specific strength at $T \leq 800$°C (Fig. 1a) [6]. The subsequent study [8] revealed that the structure of this alloy is ordered in the B2 type (Fig. 1b), which was explained by the presence of Al and determined its excellent strength characteristics.

Owing to the single-phase structure, AlNbTiV alloy is a convenient model composition to systematically study the effect of chemical composition on the structure and mechanical properties and to search for new compositions with advanced characteristics. Cr and Zr were chosen as alloying elements [7, 8]. It was found that a small addition of Cr to AlNbTiV alloy does not change its phase composition and microstructure (Figs. 2a and 2b). However, in equiatomic AlCrNbTiV alloy and in $AlCr_{1.5}NbTiV$ alloy with the maximum chromium content we observed the precipitation of Cr- and Nb-rich hexagonal C14 Laves phase particles in the bulk of and along the boundaries of B2 grains (Figs. 2a and 2c). The addition of even a small amount of Zr to AlNbTiV alloy led to the formation of a two-phase microstructure represented by a coarse-grained parent B2 phase and Zr_5Al_3 particles (Figs. 2a and 2d). With increasing Zr content, an additional C14 Laves phase enriched in

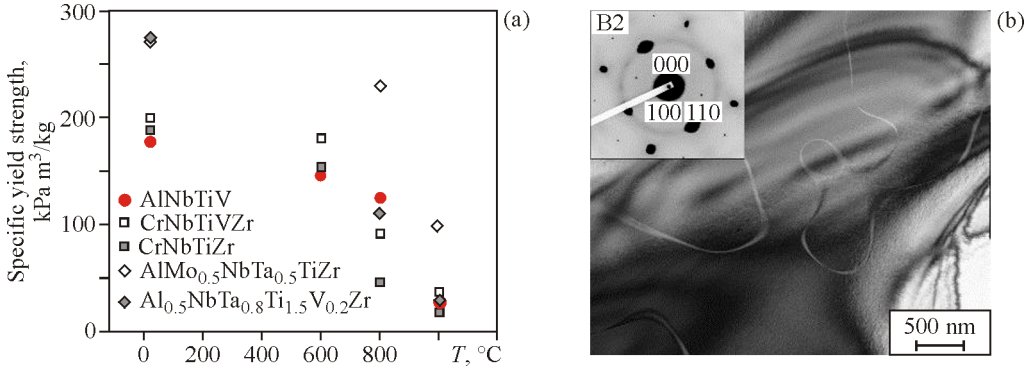

Fig. 1. Temperature dependence of the specific yield strength of AlNbTiV alloy and other refractory HEAs [4, 12] (a); bright-field image of the fine structure of AlNbTiV alloy, TEM (b).

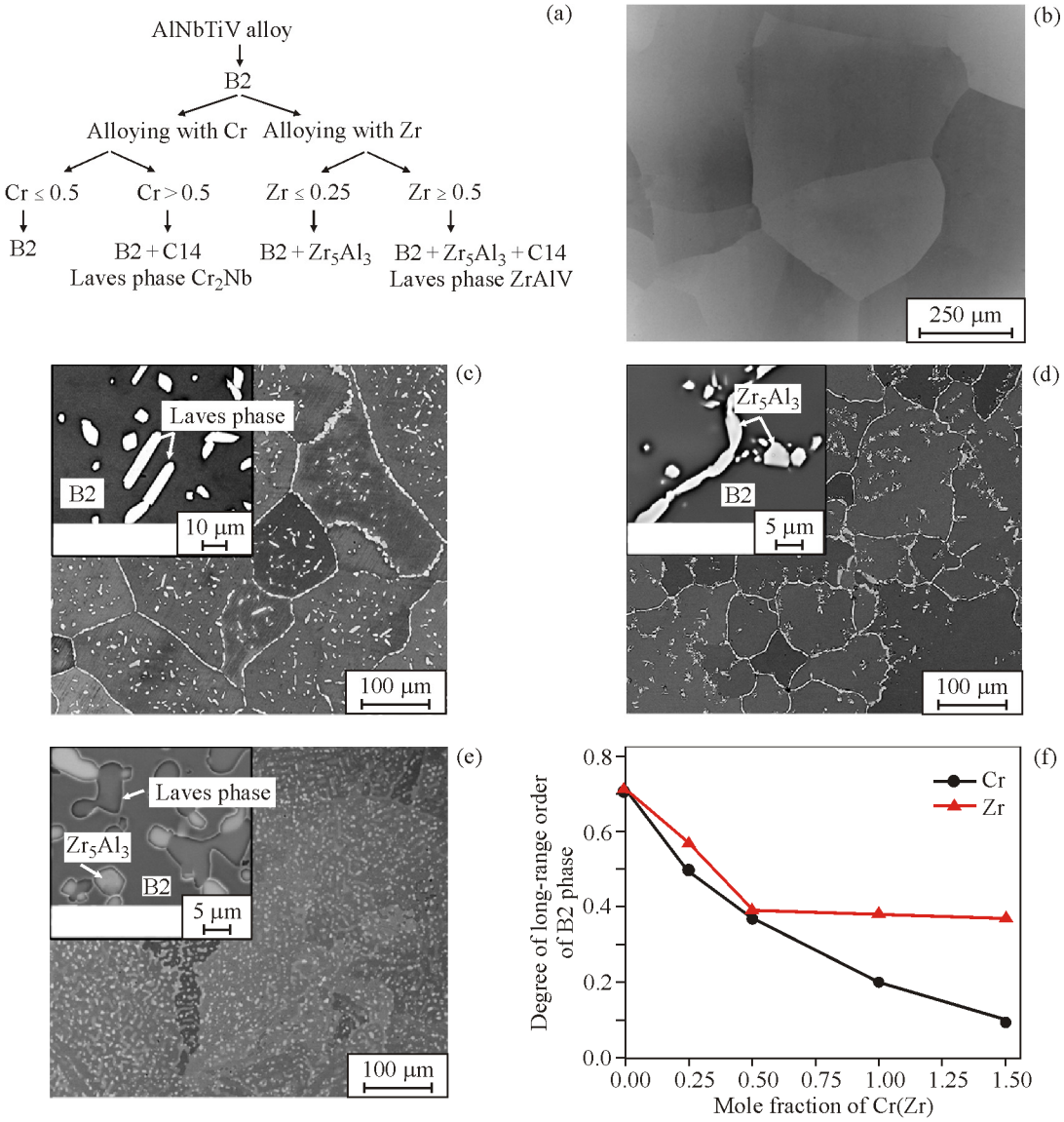

Fig. 2. A schematic illustration of the relationship between the chemical and phase composition of $AlCr_xNbTiVZr_y$ alloys (a); microstructure of $AlCr_{0.25}NbTiV$ (b), AlCrNbTiV (c), $AlNbTiVZr_{0.25}$ (d), and AlNbTiVZr (e) alloys in the initial state; the degree of long-range order of the B2 phase versus the Cr or Zr content (f) (color online).

Zr, Al, and V was formed (Figs. 2a and 2e). Cr and Zr also reduced the degree of long-range order of the B2 phase due to a decrease in the Al content (Fig. 2f).

Analysis of mechanical properties revealed that Cr and Zr increase the strength of AlNbTiV alloy at $T < 1000$°C (Figs. 3a and 3b). Cr caused an almost linear increase in yield strength at 22 and 600°C (Fig. 3a). Zr led to a more pronounced hardening effect at lower concentrations, but at higher Zr contents the effect on the yield strength was weaker at 22 and 600°C (Fig. 3b). A more complex relationship between strength and chemical composition was observed at 800°C (Figs. 3a and 3b). The analysis showed that Cr and Zr enhance the strength at $T <$ 1000°C due to solid solution strengthening and formation of second-phase particles. The complex dependence of the yield strength on the alloying element content at 800°C can be associated with a change in the degree of ordering of the B2 phase (Fig. 2f).

Alloying with Cr or Zr significantly improved both the absolute as well as the specific strength of the initial AlNbTiV alloy (Fig. 3e). Some compositions demonstrated a higher specific yield strength at $T \leq 800$°C compared to iron-chromium-nickel alloys EP718 and EK2, and nickel superalloys Inconel 706,

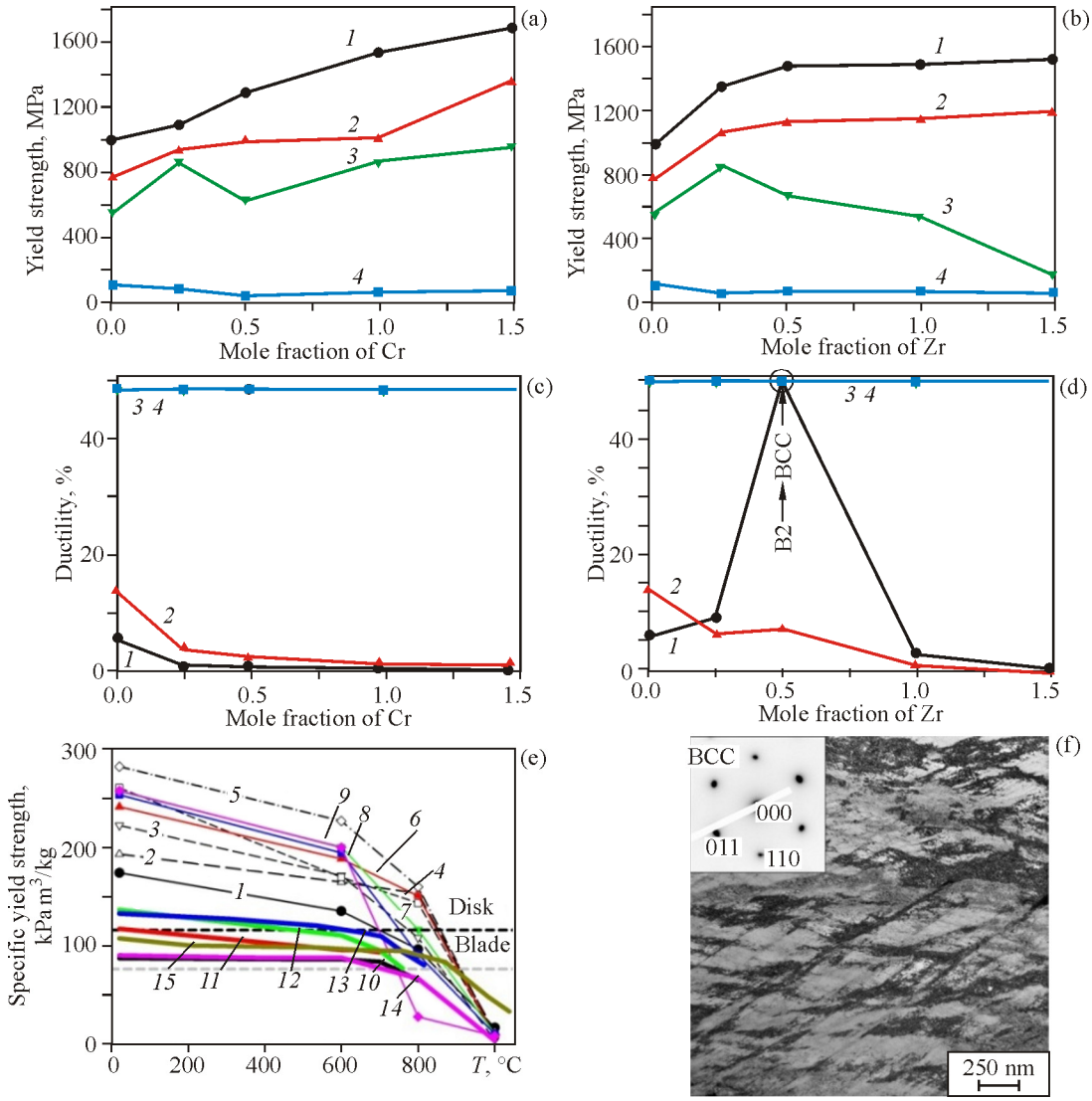

Fig. 3. Temperature dependences of yield strength (a, b) and ductility (c, d) for different Cr (a, c) or Zr contents (b, d); temperature dependence of the specific yield strength of $AlCr_xNbTiVZr_y$ alloys, iron-chromium-nickel alloys EP718 and EK2 [13], nickel superalloys Inconel 706 [14], Inconel 718 [15], Nimonic 80A [16], and Mar-M247 [17] (e); microstructure of AlNbTiV $Zr_{0.5}$ alloy after uniaxial compression at $T = 22$°C to 50% strain, TEM (f). a–d—22 (*1*), 600 (*2*), 800 (*3*), 1000°C (*4*); e—AlNbTiV (*1*), $AlCr_{0.25}NbTiV$ (*2*), $AlCr_{0.5}NbTiV$ (*3*), AlCrNbTiV (*4*), $AlCr_{1.5}NbTiV$ (*5*), $AlNbTiVZr_{0.25}$ (*6*), $AlNbTiVZr_{0.5}$ (*7*), AlNbTiVZr (*8*), $AlNbTiVZr_{1.5}$ (*9*), EP718 (*10*), EK2 (*11*), Inconel 706 (*12*), Inconel 718 (*13*), Nimonic 80A (*14*), Mar M247 (*15*) (color online).

Inconel 718, Nimonic 80A and Mar-M247 used for the manufacture of gas turbine components (blades, rings, disks) (Fig. 3e) [13–17]. The Cr-containing alloys $AlCr_{0.25}NbTiV$, AlCrNbTiV, and $AlCr_{1.5}NbTiV$ had the highest specific yield strength (more than 150 kPa m^3/kg) at $T = 800$°C. Among Zr-containing alloys, only one composition $AlNbTiVZr_{0.25}$ reached a comparable specific strength.

However, alloys intended to replace existing structural materials should have a balance of mechanical properties. AlNbTiV alloy initially had limited ductility at $T < 800$°C due to the ordered structure. Alloying with Cr led to a further deterioration of this characteristic at 22 and 600°C (Fig. 3c). A small addition of Zr had a positive effect (Fig. 3d). In particular, $AlNbTiVZr_{0.25}$ alloy showing the highest strength at 800°C had about 10% ductility. $AlNbTiVZr_{0.5}$ could be strained up to 50% relative strain without fracture, due to deformation-induced disordering of the parent B2 phase (Figs. 3d and 3f). A likely reason for the reduced ductility of single-phase Cr-containing composites, compared to alloys with Zr, could be a higher concentration of valence electrons [18]. Additionally, the ductility of the alloys

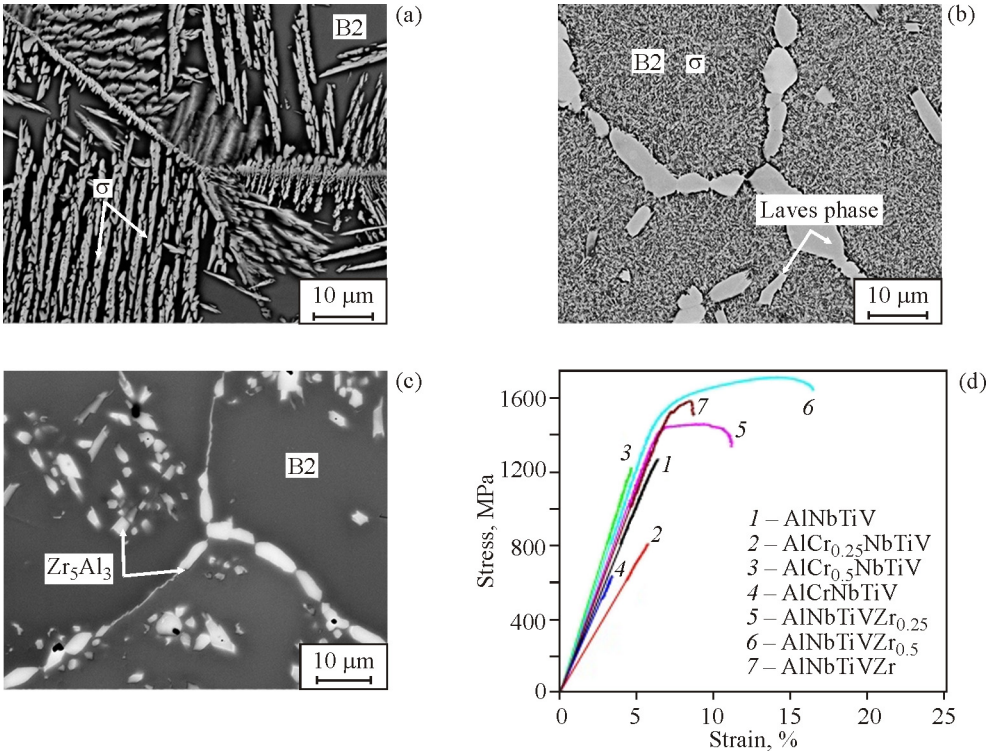

Fig. 4. Microstructure of AlNbTiV (a), AlCrNbTiV (b), and $AlNbTiVZr_{0.25}$ (c) alloys after annealing at 800°C for 100 h; mechanical properties of $AlCr_xNbTiVZr_y$ alloys annealed at 800°C for 100 h at $T = 22$°C (d) (color online).

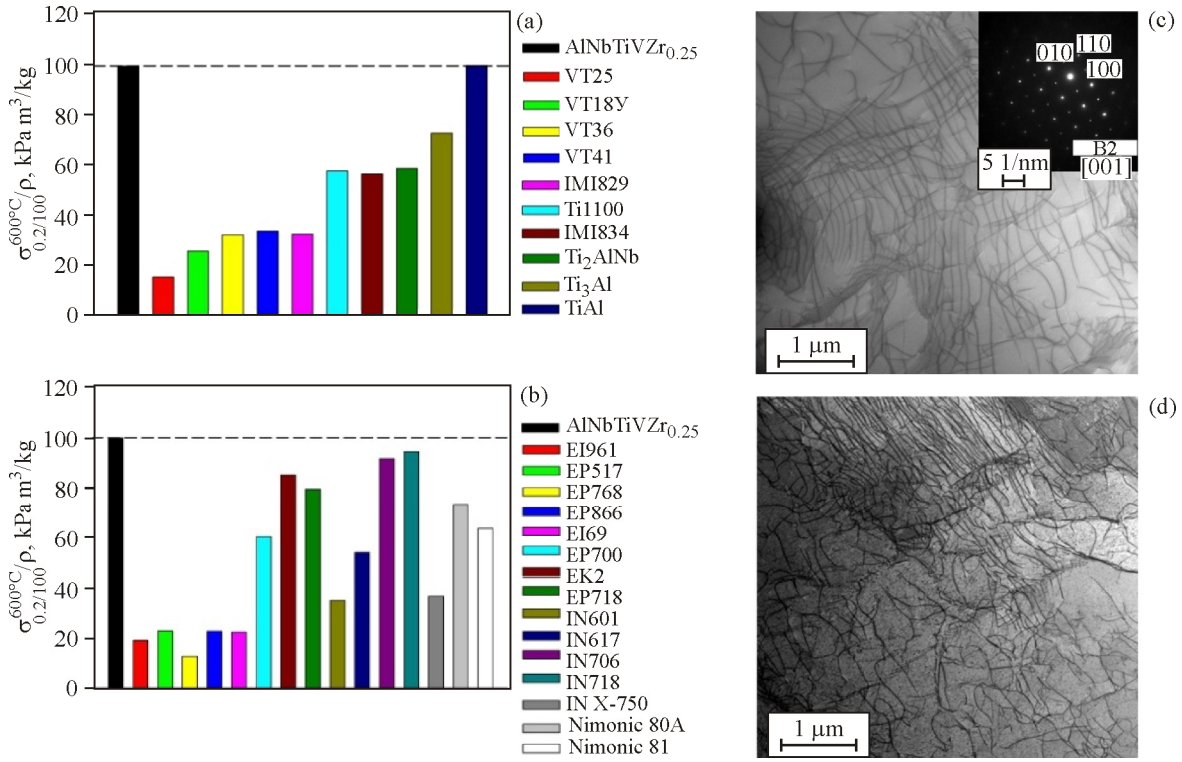

Fig. 5. Comparison of the specific creep limits of $AlNbTiVZr_{0.25}$ alloy, iron-chromium-nickel and nickel superalloys, high-temperature titanium alloys, α_2-Ti_3Al, ortho-Ti_2AlNb, and γ-TiAl alloys (a, b); structure of $AlNbTiVZr_{0.25}$ alloy after creep strength tests at $T = 800$°C at a stress of 100 (c) and 325 MPa (d) (color online).

at $T < 800$°C was noticeably affected by the second-phase particles and the degree of ordering of the B2 phase (Fig. 2f).

One of the most important characteristics of high-temperature materials is the stability of their structure and properties during long-term operation at potential operating temperatures. By studying the structural-phase stability and mechanical properties of AlNbTiV alloy and Cr-containing compositions annealed at $T = 800$ or 1000°C for 100 h, we found the formation of a σ phase enriched in Nb and Al (Figs. 4a and 4b) which led to microhardness increase and embrittlement (Fig. 4d) [9]. In Zr-doped alloys, the structure and mechanical properties remained relatively stable (Figs. 4c and 4d).

For $AlNbTiVZr_{0.25}$ alloy, which showed the best combination of high specific strength at $T \leq 800$°C, acceptable ductility, stable structure and properties, we also studied the creep resistance. According to test results, the specific creep limit of $AlNbTiVZr_{0.25}$ alloy at $T = 600$°C surpasses the creep limit of well known domestic and foreign high-temperature and intermetallic titanium alloys (Fig. 5a), as well as iron-chromium-nickel and nickel superalloys (Fig. 5b).

Using $AlNbTiVZr_{0.25}$ alloy as an example, we studied for the first time the creep mechanisms of refractory HEAs. A detailed examination of the fine microstructure after testing at $T = 800$°C at stresses of 100 and 325 MPa revealed a uniform distribution of dislocations, with the formation of subgrain boundaries but without a developed substructure (Figs. 5c and 5d). It was found that the main creep mechanism of $AlNbTiVZr_{0.25}$ alloy at $T = 800$°C was the viscous glide of dislocations resulting from their interaction with the atmospheres of the atoms of the constituent elements.

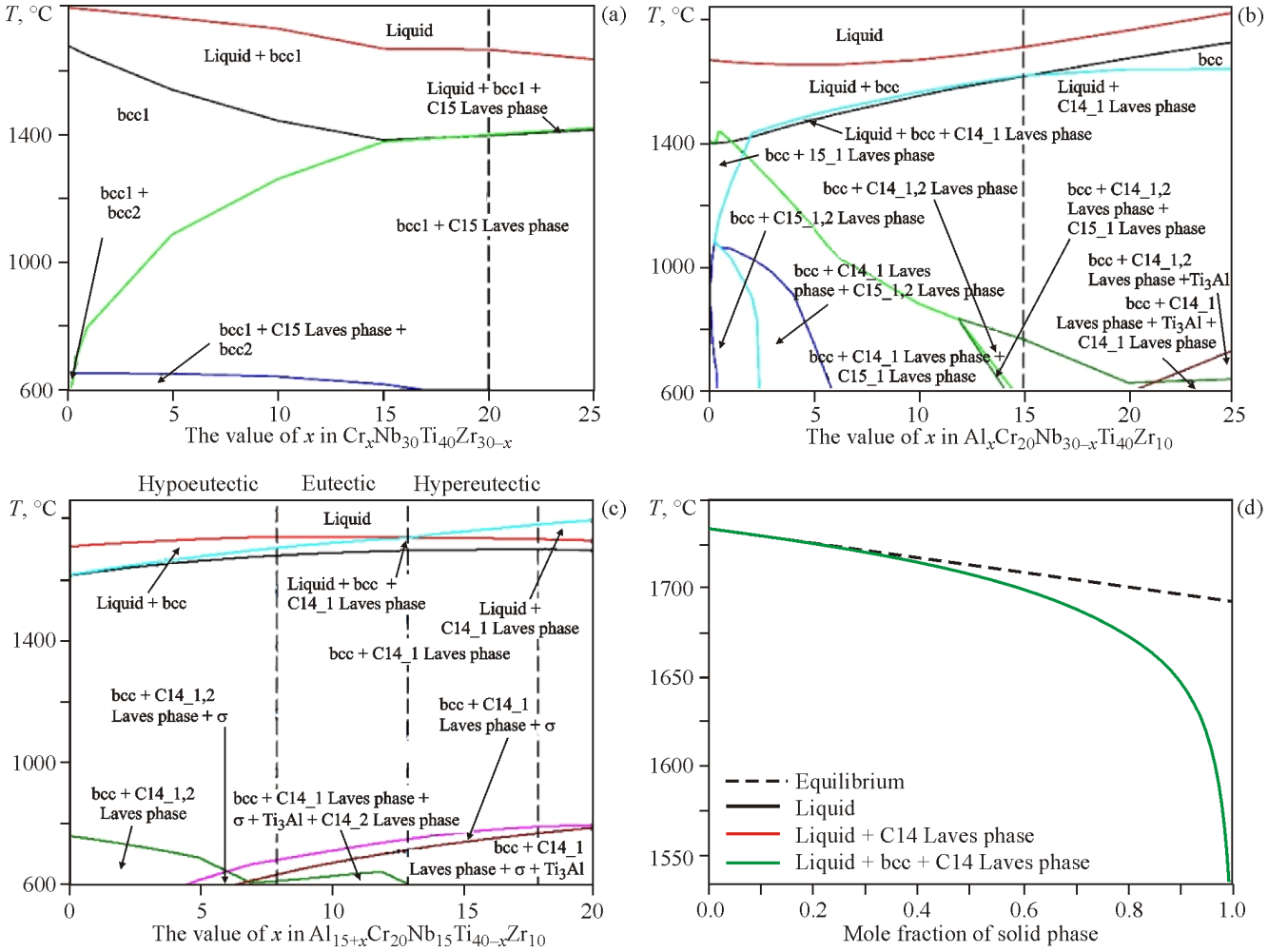

Fig. 6. Quasi-binary phase diagrams of $Cr_xNb_{15}Ti_{40}Zr_{30-x}$ (a), $Al_xCr_{20}Nb_{30-x}Ti_{40}Zr_{10}$ (b), and $Al_{15+x}Cr_{20}Nb_{15}Ti_{40-x}Zr_{10}$ (c); non-equilibrium crystallization of $Al_{28}Cr_{20}Nb_{15}Ti_{27}Zr_{10}$ alloy according to the Scheil–Gulliver model (d).

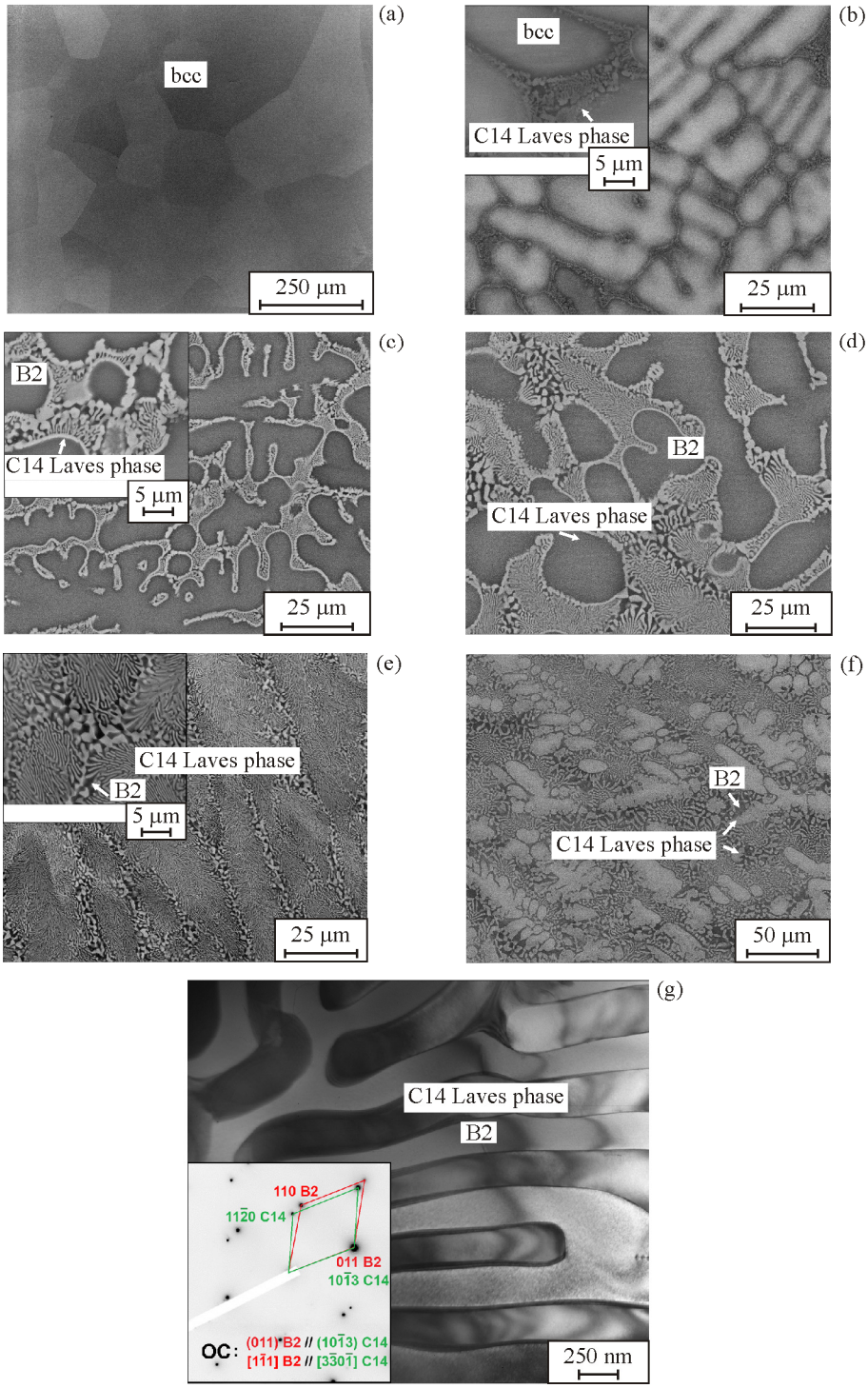

Fig. 7. Microstructure of $Nb_{30}Ti_{40}Zr_{30}$ (a), $Cr_{20}Nb_{30}Ti_{40}Zr_{10}$ (b), $Al_{15}Cr_{20}Nb_{15}Ti_{40}Zr_{10}$ (c), $Al_{23}Cr_{20}Nb_{15}Ti_{32}Zr_{10}$ (d), $Al_{28}Cr_{20}Nb_{15}Ti_{27}Zr_{10}$ (e, g), and $Al_{33}Cr_{20}Nb_{15}Ti_{22}Zr_{10}$ alloys (f): SEM (a–f) and TEM (g).

3.2. Development and Investigation of Al-Cr-Nb-Ti-Zr Eutectic Alloys

Despite the remarkable properties of AlNbTiV$Zr_{0.25}$ alloy, it is nevertheless interesting to see whether such alloys can be further improved by controlling their microstructure. An attractive way to increase the heat resistance while maintaining acceptable ductility is to create composite structures

with a regular arrangement of soft and hard phases, which can be done, e.g., in eutectic alloys [19, 20]. Eutectic alloys generally have a stable structure, a good combination of strength and ductility, and good casting properties. However, in contrast to 3d-transition-metal HEAs in which eutectic structures are often observed and whose compositions can be predicted by various well-developed methods, refractory HEAs with such a microstructure are extremely rare.

The potential of eutectic refractory HEAs as advanced high-temperature materials was studied using the CALPHAD method (CALculation of PHAse Diagrams) on a number of alloys of the Al-Cr-Nb-Ti-Zr system [11]. The alloys were designed by analyzing equilibrium and nonequilibrium phase diagrams in several stages: from the determination of single-phase composition of $Nb_{30}Ti_{40}Zr_{30}$ to the description of a eutectic reaction in quasi-binary system $Al_{15+x}Cr_{20}Nb_{15}Ti_{40-x}Zr_{10}$ (Fig. 6).

An experimental study showed that thermodynamic modeling is an effective tool for the development of eutectic refractory HEAs. CALPHAD accurately predicted the microstructure and phase composition of $Nb_{30}Ti_{40}Zr_{30}$ (Fig. 7a) and $Cr_{20}Nb_{30}Ti_{40}Zr_{10}$ (Fig. 7b) alloys. Despite the fact that it cannot predict B2 ordering and underestimates the volume fraction of the Laves phase, thermodynamic modeling provided correct information about the type of micro-

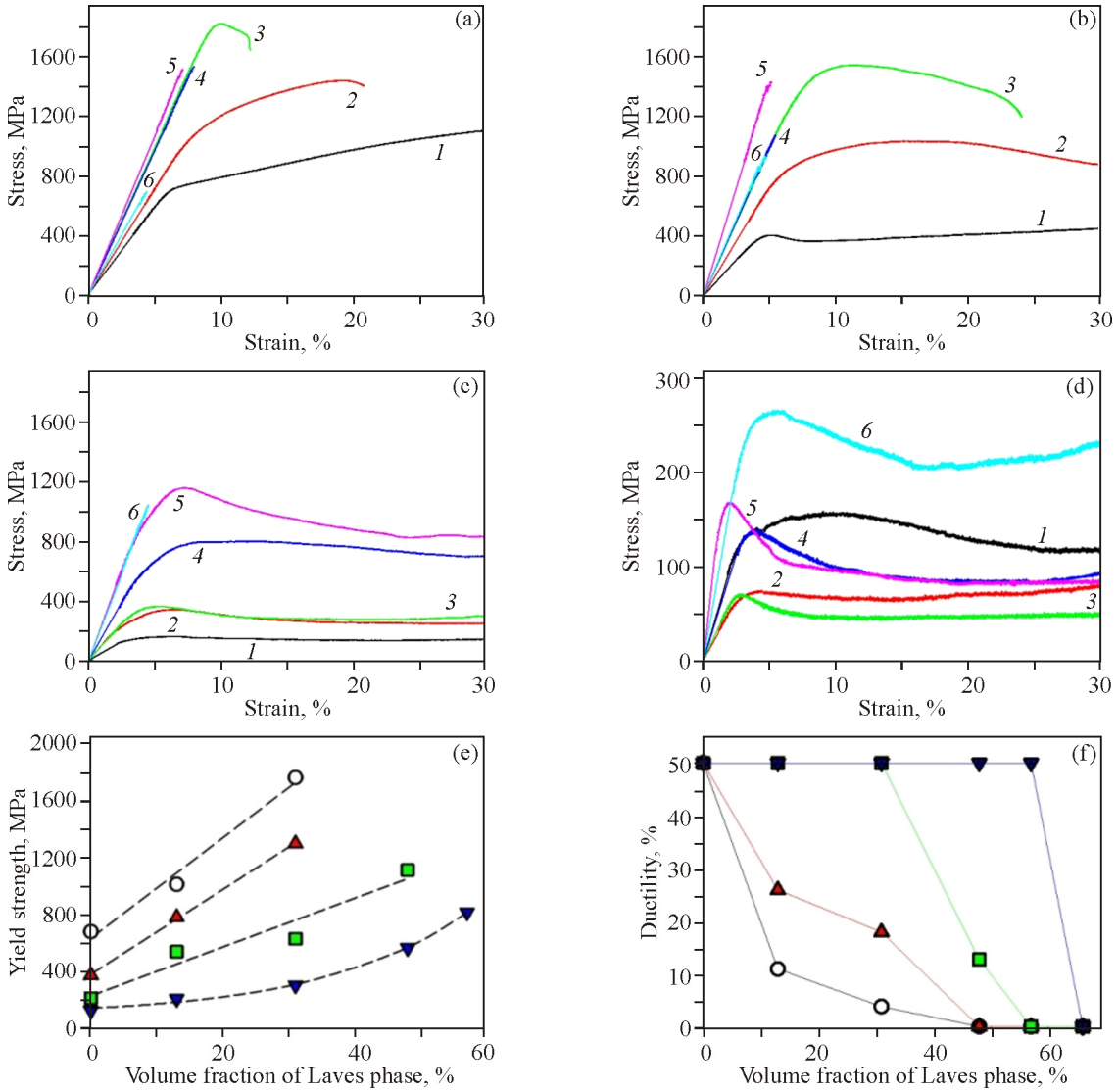

Fig. 8. Stress–strain curves of $Nb_{30}Ti_{40}Zr_{30}$ (*1*), $Cr_{20}Nb_{30}Ti_{40}Zr_{10}$ (*2*), $Al_{15}Cr_{20}Nb_{15}Ti_{40}Zr_{10}$ (*3*), $Al_{23}Cr_{20}Nb_{15}Ti_{32}Zr_{10}$ (*4*), $Al_{28}Cr_{20}Nb_{15}Ti_{27}Zr_{10}$ (*5*), $Al_{33}Cr_{20}Nb_{15}Ti_{22}Zr_{10}$ alloys (*6*) obtained during uniaxial compression at 22 (a), 600 (b), 800 (c), and 1000°C (d); the yield strength (e) and ductility (f) of alloys versus the volume fraction of the Laves phase: 22 (○), 600 (▲), 700 (■), and 1800°C (▼) (color online).

structures in alloys with Al (Figs. 7c–7g). The transition from single-phase to eutectic structures was induced by an increase in the volume fraction of the Laves phase. Analysis of binary and ternary systems showed that the eutectic structure of $Al_{28}Cr_{20}Nb_{15}Ti_{27}Zr_{10}$ alloy consisting of the B2 phase and C14 Laves phase (Figs. 7e and 7g) can be obtained only due to the multicomponent nature of HEAs. Moreover, the formation of such a eutectic microstructure was energetically favorable because of the unique orientation relationship $(011)_{B2} \parallel (10\bar{1}3)_{C14}$, $[1\bar{1}1]_{B2} \parallel [3\bar{3}0\bar{1}]_{C14}$ [21] that provides good crystallographic relationship between the phases.

Results of mechanical uniaxial compression tests conducted at 22, 600, 700, 800, and 1000°C on single-phase $Nb_{30}Ti_{40}Zr_{30}$ alloy showed its low room-temperature strength (675 MPa) and high ductility (>50%) (Fig. 8a). An increase in the test temperature had no effect on ductility, but led to a noticeable decrease in strength (Figs. 8b–8d). The Laves phase formation as a result of subsequent alloying strongly influenced the mechanical properties of the alloys (Figs. 8a–8d). From the viewpoint of strength, the Laves phase served as an effective strengthening component of the studied alloys. At temperatures up to 700°C, there was a linear relationship between the yield strength and the volume fraction of the Laves phase (Fig. 8e). A test temperature increase to 800°C led to a more complex relationship. According to the obtained dependence, the Laves phase strengthening at 800°C became dominant only with a volume fraction of more than 31%: the strength increased exponentially above this value. The exponential growth of strength (from 125 to 810 MPa) at 800°C in the studied alloys was a result of the transition from a single-phase structure to a eutectic one. On the other hand,

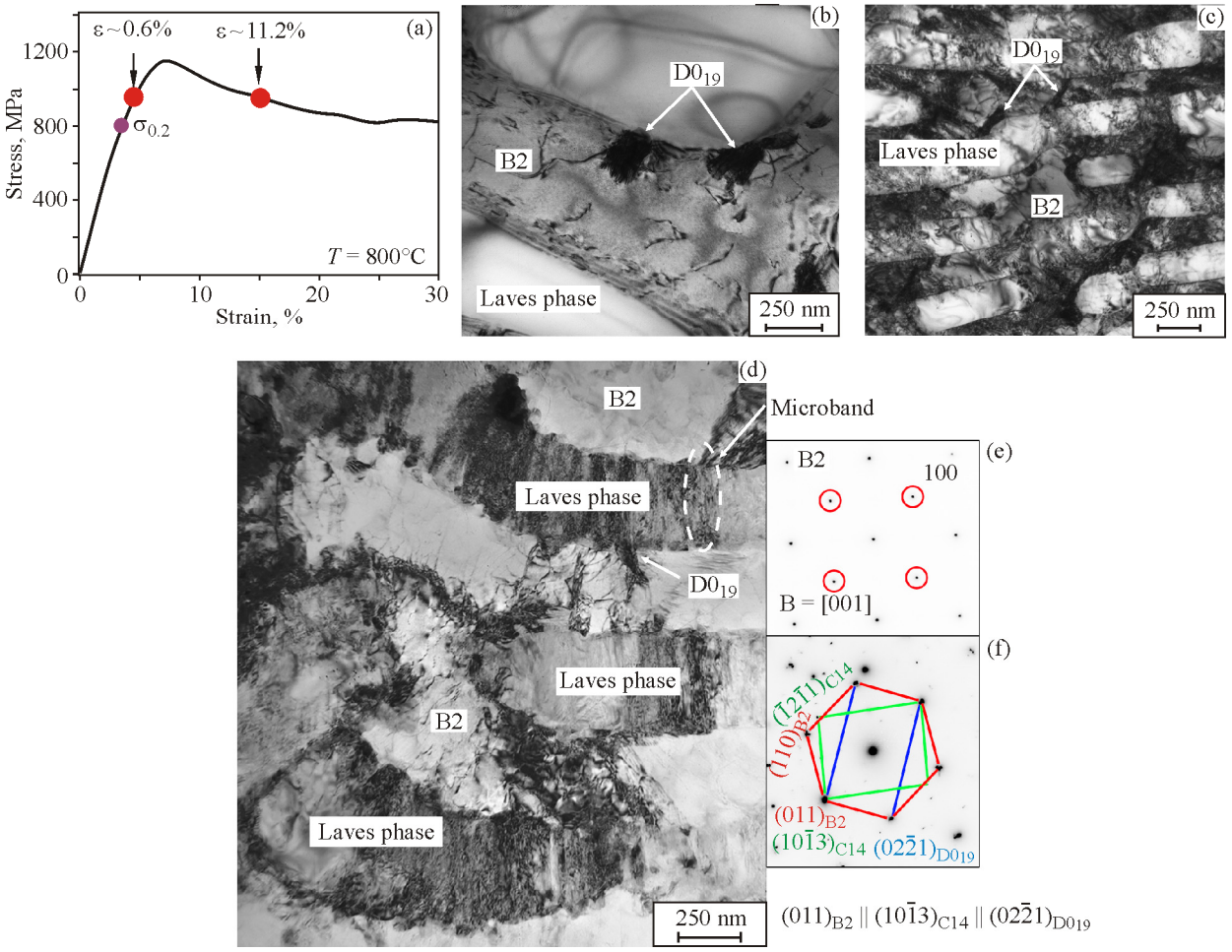

Fig. 9. Stress–strain curve plotted during uniaxial compression of $Al_{28}Cr_{20}Nb_{15}Ti_{27}Zr_{10}$ eutectic alloy at 800°C to different strains (a); TEM images of the microstructure of $Al_{28}Cr_{20}Nb_{15}Ti_{27}Zr_{10}$ eutectic alloy after 0.6 (b), 11.2 (c), and 50% (d) relative deformation at 800°C; e, f—electron diffraction patterns taken from the B2 phase (e) and simultaneously from the B2, Laves C14 and $D0_{19}$ phases (f) in Fig. 9d.

the strength of all two-phase alloys sharply decreased with temperature rise to 1000°C (Fig. 8d), which is evidently explained by the occurrence of phase transformations, recovery, and recrystallization.

The Laves phase not only increased the strength but also sharply reduced the ductility (Figs. 8a–8d and 8f). Only hypoeutectic alloys with an up to 31% volume fraction of the Laves phase exhibited some ductility at room temperature. Alloys with a 48–66% volume fraction of the Laves phase, such as $Al_{23}Cr_{20}Nb_{15}Ti_{32}Zr_{10}$ hypoeutectic, $Al_{28}Cr_{20}Nb_{15}Ti_{27}Zr_{10}$ eutectic, and $Al_{33}Cr_{20}Nb_{15}Ti_{22}Zr_{10}$ hypereutectic alloys, were brittle up to temperatures of 700–1000°C.

For a deeper understanding of the mechanical behavior of multiphase refractory HEAs, we studied the microstructural evolution of $Al_{28}Cr_{20}Nb_{15}Ti_{27}Zr_{10}$ eutectic alloy subjected to uniaxial compression at 800°C (Fig. 9). It was shown that plastic deformation at the hardening stage ($\varepsilon \approx 0.6\%$ in Fig. 9a) occurs by the glide of dislocations in the soft B2 phase (Fig. 9b). After reaching the maximum value, the yield stresses decreased significantly ($\varepsilon \approx 11.2\%$ in Fig. 9a) due to the onset of plastic deformation in the solid C14 Laves phase (Fig. 9c). At large strains ($\varepsilon = 50\%$), we observed a rapid formation of a substructure in the B2 phase, which remained ordered (Fig. 9e), and the formation of perpendicular microbands inside curved C14 Laves lamellae (Fig. 9d). The lamellar structure was highly stable to fragmentation and/or globularization during high-temperature deformation due to the stability of the previously found orientation relationship between the B2 and C14 Laves phases, as a result of which low-energy interphase boundaries were preserved.

Deformation of $Al_{28}Cr_{20}Nb_{15}Ti_{27}Zr_{10}$ eutectic alloy at 800°C also led to the precipitation of a new phase with an ordered hcp ($D0_{19}$) structure in B2 lamellas near the B2/C14 Laves phase interfaces (Figs. 9b–9d). The following orientation relationship was found between the three phases (Fig. 9f):

$$(011)_{B2} \parallel (10\bar{1}3)_{C14} \parallel (0\bar{2}21)_{D019}.$$

With strain increase, the morphology of $D0_{19}$ particles transformed into a needle-shaped one and they effectively divided the B2 lamellae.

It is surmised that heat treatment can produce a three-phase B2/C14 Laves/$D0_{19}$ structure to provide even higher strength at elevated temperatures. The ductility of eutectic compositions can be improved by changing the degree of ordering of the parent B2 phase by reducing the Al concentration [8, 22]. The creep and oxidation resistance of the synthiesized eutectic alloys should be studied in order to more accurately assess their application potential as refractory and high-temperature materials.

4. CONCLUSIONS

The composition/structure/properties relationships were investigated for $AlCr_xNbTiVZr_y$ high-entropy alloys ($x = 0.00$, 0.25, 0.50, 1.00, 1.50 at $y = 0$ and $y =$ 0.00, 0.25, 0.50, 1.00, 1.50 at $x = 0$). It was shown that alloying with Cr or Zr enhances the strength of AlNbTiV alloy with a single-phase B2 structure due to the formation of second-phase particles, solid solution strengthening, and a change in the degree of ordering of the parent B2 phase. The specific strength of some compositions significantly exceeded that of industrial nickel superalloys at $T \leq 800$°C. Zr-containing alloys showed higher ductility as well as better structural stability and properties. AlNbTiV $Zr_{0.25}$ alloy surpassed industrial high-temperature alloys in the specific creep limit at $T = 600$°C.

New Al-Cr-Nb-Ti-Zr alloys with a unique eutectic structure consisting of the B2 and C14 Laves phases were designed by thermodynamic modeling. It was found that the formation of such a microstructure is energetically favorable as a result of a specific orientation relationship between the phases. The transition from a single-phase bcc structure to a eutectic B2/C14 structure greatly increased the strength but reduced the ductility. High-temperature deformation of $Al_{28}Cr_{20}Nb_{15}Ti_{28}Zr_{10}$ eutectic alloy proceeded in stages: from dislocation glide in the soft B2 phase at the stage of hardening to the involvement of the hard Laves phase in plastic flow at the stage of softening, and collective deformation of both phases at the steady-state stage. The lamellar eutectic structure of the alloy was highly stable to fragmentation and/or globularization due to the preservation of the initial orientation relationship and the precipitation of $D0_{19}$ particles.

The results reported in this study can be useful for the development of new refractory HEAs with improved properties for potential applications as high-temperature materials.

FUNDING

This work was financially supported by the Russian Science Foundation (Project No. 19-79-30066). The authors are grateful to the staff of the Common Use Center “Technologies and Materials” of NRU BelSU for assistance in conducting research, and express gratitude to M.A. Tikhonovsky, D.G. Shaysultanov, A.O. Semenyuk, and S.V. Zherebtsov.

REFERENCES

1. Senkov, O.N., Wilks, G.B., Miracle, D.B., Chuang, C.P., and Liaw, P.K., Refractory High-Entropy Alloys, *Intermetallics*, 2010, vol. 9, no. 18, pp. 1758–1765. https://doi.org/10.1016/j.intermet.2010.05.014
2. Senkov, O.N., Wilks, G.B., Scott, J.M., and Miracle, D.B., Mechanical Properties of $Nb_{25}Mo_{25}Ta_{25}W_{25}$ and $V_{20}Nb_{20}Mo_{20}Ta_{20}W_{20}$ Refractory High Entropy Alloys, *Intermetallics*, 2011, vol. 5, no. 19, pp. 698–706. https://doi.org/10.1016/j.intermet.2011.01.004
3. Senkov, O.N., Senkova, S.V., Woodward, C., and Miracle, D.B., Low-Density, Refractory Multi-Principal Element Alloys of the Cr-Nb-Ti-V-Zr System: Microstructure and Phase Analysis, *Acta Mater*., 2013, vol. 61, no. 5, pp. 1545–1557. https://doi.org/10.1016/j.actamat.2012.11.032
4. Senkov, O.N., Senkova, S.V., Miracle, D.B., and Woodward, C., Mechanical Properties of Low-Density, Refractory Multi-Principal Element Alloys of the Cr–Nb–Ti–V–Zr System, *Mater. Sci. Eng. A*, 2013, vol. 565, pp. 51–62. https://doi.org/10.1016/j.msea.2012.12.018
5. Senkov, O.N., Senkova, S.V., and Woodward, C., Effect of Aluminum on the Microstructure and Properties of Two Refractory High-Entropy Alloys, *Acta Mater*., 2014, vol. 68, pp. 214–228. https://doi.org/10.1016/j.actamat.2014.01.029
6. Stepanov, N.D., Shaysultanov, D.G., Salishchev, G.A., and Tikhonovsky, M.A., Structure and Mechanical Properties of a Light-Weight AlNbTiV High Entropy Alloy, *Mater. Lett*., 2015, vol. 142, pp. 153–155. https://doi.org/10.1016/j.matlet.2014.11.162
7. Stepanov, N.D., Yurchenko, N.Yu., Skibin, D.V., Tikhonovsky, M.A., and Salishchev, G.A., Structure and Mechanical Properties of the $AlCr_xNbTiV$ ($x = 0.0$, 0.5, 1.0, 1.5) High Entropy Alloys, *J. Alloy. Compd*., 2015, vol. 652, pp. 266–280. https://doi.org/10.1016/j.jallcom.2015.08.224
8. Yurchenko, N.Y., Stepanov, N.D., Zherebtsov, S.V., Tikhonovsky, M.A., and Salishchev, G.A., Structure and Mechanical Properties of B2 Ordered Refractory $AlNbTiVZr_x$ ($x = 0$–1.5) High-Entropy Alloys, *Mater. Sci. Eng. A*, 2017, vol. 704, pp. 82–90. https://doi.org/10.1016/j.msea.2017.08.019
9. Yurchenko, N.Y., Stepanov, N.D., Gridneva, A.O., Mishunin, M.V., Salishchev, G.A., and Zherebtsov, S.V., Effect of Cr and Zr on Phase Stability of Refractory Al-Cr-Nb-Ti-V-Zr High-Entropy Alloys, *J. Alloy. Compd*., 2018, vol. 757, pp. 403–414. https://doi.org/10.1016/j.jallcom.2018.05.099
10. Kral, P., Blum, W., Dvorak, J., Yurchenko, N., Stepanov, N., Zherebtsov, S., Kuncicka, L., Kvapilova, M., and Sklenicka, V., Creep Behavior of an AlTiV $NbZr_{0.25}$ High Entropy Alloy at 1073 K, *Mater. Sci. Eng. A*, 2020, vol. 783, p. 139291. https://doi.org/10.1016/j.msea.2020.139291
11. Yurchenko, N., Panina, E., Zherebtsov, S., and Stepanov, N., Design and Characterization of Eutectic Refractory High Entropy Alloys, *Materialia*, 2021, vol. 16, p. 101057. https://doi.org/10.1016/j.mtla.2021.101057
12. Senkov, O.N., Woodward, C., and Miracle, D.B., Microstructure and Properties of Aluminum-Containing Refractory High-Entropy Alloys, *JOM*, 2014, vol. 66, pp. 2030–2042. https://doi.org/10.1007/s11837-014-1066-0
13. Kishkin, S.T., Kachalov, E.B., and Bulygin, I.P., *Heat-Resistant Steels and Alloys. Alloys Based on Refractory Metals*, Shalin, R.A., Ed., ONTI, 1989.
14. INCONEL alloy 706, *Spec. Met. Corporation*, 2007, pp. 1–12.
15. INCONEL alloy 718, *Spec. Met. Corporation*, 2007, pp. 13–28.
16. NIMONIC alloy 80A, *Spec. Met. Corporation*, 2004, pp. 1–24.
17. Kaufman, M., Properties of Cast MAR-M-247 for Turbine Blisk Applications, in *Superalloys: V International Symposium*, 1984, pp. 43–52.
18. Sheikh, S., Shafeie, S., Hu, Q., Ahlstrom, J., Persson, C., Vesely, J., Zyka, J., Klement, U., and Guo, S., Alloy Design for Intrinsically Ductile Refractory High-Entropy Alloys, *J. Appl. Phys*., 2016, vol. 120, p. 164902. https://doi.org/10.1063/1.4966659
19. Thompson, E.R. and George, F.D., Eutectic Superalloys, in *SAE Technical Papers*, 1969, pp. 2283–2288.
20. Lu, Y., Dong, Y., Jiang, H., Wang, Z., Cao, Z., Guo, S., Wang, T., Li, T., and Liaw, P.K., Promising Properties and Future Trend of Eutectic High Entropy Alloys, *Scripta Mater*., 2020, vol. 187, pp. 202–209. https://doi.org/10.1016/j.scriptamat.2020.06.022
21. Zhang, M.X. and Kelly, P.M., Edge-to-Edge Matching and Its Applications: Part I. Application to the Simple HCP/BCC System, *Acta Mater*., 2005, vol. 53, pp. 1073–1084. https://doi.org/10.1016/j.actamat.2004.11.007
22. Laube, S., Chen, H., Kauffmann, A., Schellert, S., Muller, F., Gorr, B., Muller, J., Butz, B., Christ, H.-J., and Heilmaier, M., Controlling Crystallographic Ordering in Mo–Cr–Ti–Al High Entropy Alloys to Enhance Ductility, *J. Alloy. Compd*., 2020, vol. 823, p. 153805. https://doi.org/10.1016/j.jallcom.2020.153805